Published in final edited form as:
J Solution Chem. 2015 October ; 44(11): 2179–2193. doi:10.1007/s10953-015-0401-6.

Molecular Dynamics Evaluation of Dielectric-Constant Mixing Rules for H_2O-CO_2 at Geologic Conditions

Raymond D. Mountain[1] and **Allan H. Harvey**[2]

[1]Chemical Sciences Division, National Institute of Standards and Technology, 100 Bureau Drive, Gaithersburg, MD 20899, raymond.mountain@nist.gov

[2]Applied Chemicals and Materials Division, National Institute of Standards and Technology, 325 Broadway, Boulder, CO 80305, 303-497-3555

Abstract

Modeling of mineral reaction equilibria and aqueous-phase speciation of C-O-H fluids requires the dielectric constant of the fluid mixture, which is not known from experiment and is typically estimated by some rule for mixing pure-component values. In order to evaluate different proposed mixing rules, we use molecular dynamics simulation to calculate the dielectric constant of a model H_2O–CO_2 mixture at temperatures of 700 K and 1000 K at pressures up to 3 GPa.

We find that theoretically based mixing rules that depend on combining the molar polarizations of the pure fluids systematically overestimate the dielectric constant of the mixture, as would be expected for mixtures of nonpolar and strongly polar components. The commonly used semiempirical mixing rule due to Looyenga works well for this system at the lower pressures studied, but somewhat underestimates the dielectric constant at higher pressures and densities, especially at the water-rich end of the composition range.

Keywords

carbon dioxide; dielectric constant; geochemistry; mixtures; relative permittivity; water

1 Introduction

The static dielectric constant (relative permittivity) is a key quantity in continuum descriptions of the thermodynamics of ions in solution. In geochemistry, the dielectric constant of water appears in the Born contribution to Gibbs energies of ionic species in the widely used Helgeson-Kirkham-Flowers (HKF) approach to aqueous thermodynamics [1-7]. The uses and limitations of such models have recently been reviewed by Dolejš [8]. This approach has proven useful in estimating equilibrium constants and other thermodynamic properties that are essential in modeling the distribution and transport of components between minerals and fluids. However, its range of application has been limited in pressure

---

(corresponding author) Allan H. Harvey, aharvey@boulder.nist.gov.

(to 0.5 GPa) and to conditions where the solvent can be assumed to be H_2O with the amount of dissolved gas or other solutes too small to significantly affect the dielectric constant.

Recently, there has been interest in extending these methods to conditions of the deep crust and upper mantle [8-12]. Aqueous fluids at these conditions would typically have a large fraction of H_2O, but would also have significant fractions of other species such as CO_2 and CH_4 [13-16]. Some modeling studies have examined the effect of the temperature, pressure, and composition dependence of the dielectric constant of these high-pressure mixed fluids on mineral reaction equilibria and speciation in the aqueous phase [9,17-19]. The paper of Galvez et al. [19] was to our knowledge the first to examine in detail the effects of dielectric mixing rules on calculated equilibria at these conditions, but they had no way to evaluate the accuracy of the mixing rules used.

There are no experimental measurements of mixture dielectric constants at these extreme conditions, so it is necessary to make estimates based on theory and/or on mixing extrapolated pure-component values. For pure H_2O, reasonable estimates at geologic conditions can be made; the standard formulation of the International Association for the Properties of Water and Steam (IAPWS) [20,21] extends to 873 K and 1 GPa and extrapolates reasonably to higher temperatures and pressures. Estimates have also been developed based on semiempirical extrapolation [11]. A recent study [22] used *ab initio* molecular dynamics to calculate the dielectric constant up to approximately 2000 K and 10 GPa. For nonpolar fluids such as CO_2 and CH_4, the Clausius-Mosotti relationship can be used to extrapolate correlations based on reliable measurements [23] to more extreme conditions, provided that a reliable equation of state (EOS) exists to calculate the density as a function of temperature and pressure.

For mixtures, however, the situation is much less clear. It is logical to obtain the mixture dielectric constant εmix at temperature T and pressure p from some weighted combination of the pure-component values, but there is no consensus on the best approach. It has been common in geochemistry to use a mixing rule attributed to Looyenga [24,25]:

$$\varepsilon_{\text{mix}}=\left(\sum_i \Phi_i \varepsilon_1^{1/3}\right)^3, \quad (1)$$

where $\Phi_i=x_i v_i/\sum_j x_j v_j$ is the volume fraction of component i (based on pure-component molar volumes v_i at T and p) and ε_i is its dielectric constant at T and p. However, Looyenga's equation is derived for heterogeneous dispersions with small differences among ε_i. Neither of these assumptions is correct for the aqueous mixtures of interest in geologic settings, making the use of Eq. 1 for such systems questionable.

In the theory of electric polarization (see for example Böttcher [26]), the physically significant variable is not the dielectric constant itself, but rather the dielectric polarization. A convenient quantity to work with is the dielectric polarization per unit volume, which is the molar polarization ([P] in Böttcher's notation) divided by the molar volume; we will write this quantity as P and refer to it as the "polarization" for short. There is no rigorous general relationship between ε and P. However, for polar fluids (or mixtures containing polar components), a relationship due to Kirkwood [27] is widely and successfully used:

$$P_{\mathrm{K}}=\frac{(\varepsilon-1)(2\varepsilon+1)}{9\varepsilon}. \quad (2)$$

A well-established way to estimate the polarization of a mixture when pure-component values are available is due to Oster [28]:

$$(P/\rho)_{\mathrm{mix}}=\sum_i x_i\left(\frac{P(T,p)}{\rho(T,p)}\right)_i, \quad (3)$$

where x_i is the mole fraction of component i and ρ is the molar density. Equation 3 becomes a linear volume-fraction mixing rule if the excess volume of mixing V^{E} at (T, p) is zero;

$$P_{\mathrm{mix}}=\sum_i \Phi_i P_i(T,p) \qquad \left[V^{\mathrm{E}}=0\right]. \quad (4)$$

Equation 4, with Kirkwood's expression (Eq. 2) used to relate P to ε, was used by Wang and Anderko [29] to calculate the dielectric constants of mixtures of liquid solvents. Oster's Eq. 3 (attributed to Orlov and Smirnov [30]) was used by Akinfiev and Zotov [18] in their modeling of equilibria in hydrothermal solutions.

Harvey and Prausnitz [31] proposed a mixing rule similar to Eq. 3, but with the mixing performed not at constant pressure but rather at constant reduced density:

$$P_{\mathrm{mix}}=\sum_i \Phi_i^* P_i\left(T,\frac{\rho_{\mathrm{r,mix}}}{v_i^*}\right), \quad (5)$$

where v_i^* is a characteristic molar volume (usually taken as the critical volume) for component i, $\Phi_i^*=x_i v_i^*/\sum_j x_j v_j^*$ is a volume fraction defined with these characteristic volumes, and $\rho_{\mathrm{r,mix}}$ is the dimensionless reduced molar density of the mixture, $\rho_{r,\mathrm{mix}}=\rho_{\mathrm{mix}}\sum_i x_i v_i^*$.

Harvey and Lemmon [23] applied Eq. 5 to model the dielectric constant of mixtures of natural gas components, finding that it gave a modest improvement over Oster's rule (Eq. 3) for systems where the pure-component densities at (T, p) were widely different (for example, if one pure component was a gas and the other a liquid at those conditions). They also found that inclusion of the excess volume of mixing was essential for accurate results.

However, the assumption behind both the mixing rules of Oster and of Harvey and Prausnitz is that the contribution of each component to the polarization is unchanged upon mixing. This seems less likely to be true for mixtures such as the geologic fluids of interest here, where soluble nonpolar components will modify the hydrogen-bond structure of the water.

Harvey and Prausnitz [31] reported some cases where their mixing rule was inaccurate for polar/nonpolar liquid mixtures.

The purpose of the present work is to evaluate these mixing rules, at geologic temperatures and pressures, by molecular simulation of a model that qualitatively represents the H_2O-CO_2 mixture (ignoring complicating factors like ionization that might be present in the real system). Quantitative representation of the dielectric constant by the molecular model is not necessary for this purpose; in a “real” situation, values for the pure-component dielectric constants would be available, so the aspect to be tested is how the pure-component values combine to yield a mixture value. In this work, we test the mixing rules by simulating the static dielectric constant of molecular models for H_2O, CO_2, and their mixtures at temperatures of 700 K and 1000 K and pressures from 0.1 GPa to 3 GPa.

2 Molecular Simulation

2.1 Intermolecular Potentials

The simulations reported here make use of rigid, three-site models for H_2O and CO_2. The SPC/E model for water [32] has been shown to generate reasonable values for the dielectric constant at the elevated temperatures and pressures of interest here [22].

There have been several examinations of how well various interaction potential models for CO_2 predict thermodynamic properties at elevated temperatures and pressures [33-35]. The rigid, three-site model developed by Zhang and Duan (ZD) [33] performs well and slightly better than the TraPPE model [36] at these conditions. Further, there are, for the ZD model interacting with SPC/E water, *ab initio* based interaction parameters [37] that are more accurate than those based on the commonly used Lorentz-Berthelot [38] or Kong [39] combining rules.

Both the SPC/E and ZD potentials that are used here have the form of Lennard-Jones (12-6) plus Coulomb interactions between sites on molecule pairs. The Lennard-Jones sites are characterized by an interaction energy $\varepsilon_{\mathrm{LJ}}$ and a distance parameter σ, while the Coulomb interactions are characterized by partial charges q. The potential parameters are listed in Table 1. Note that while the special combining rule is used for H_2O-CO_2 interactions, the Lorentz-Berthelot rule is used for carbon-oxygen interactions between pairs of CO_2 molecules.

The Lennard-Jones interactions are truncated at separations equal to 1/2 the edge of the cubic simulation cell and a long-range correction for the pressure is included. The long-range part of the Coulomb interactions is determined by the Ewald summation method with conducting boundary conditions [40].

2.2 Molecular Dynamics Details

The equations of motion used in the simulations generate trajectories in the isothermal-isobaric (NPT) ensemble [41]. The equations of motion for the molecules and for the thermostats and barostat are integrated using a velocity-Verlet algorithm [42] adapted to include quaternions [43] to describe the orientational degrees of freedom of the rigid molecules. The coupling time for the thermostats controlling the translational and rotational degrees of freedom is 0.1 ps, the time for the barostat is 1.1 ps, and the time for the thermostat controlling the barostat is 0.11 ps. The time step for the integration of the equations is 1 fs. These values provide stable regulation of the pressure and temperature at the specified values as determined using 1 ps duration block averages to determine the standard uncertainty [44] in the estimates for the average values of the temperature, pressure, and volume. The standard uncertainties of these quantities are found to be less than 0.1% of the average values for all states examined.

The simulation times needed for good convergence of the dielectric constant were obtained by determining the sampling time needed for the long-time average of the square of the dipole-moment function $<\boldsymbol{M}^2>$ (see Eq. 7 below) to achieve a stable value. The simulation time for production runs for CO_2 and mixtures is 1 ns. Longer times are needed for convergence of the results for the fluctuations in the total dipole moment of water, so production runs of 3 ns are used for H_2O. Simulations are divided into blocks of 1 ps duration; the standard deviation of this set of results is used to obtain the standard uncertainty of calculated values.

The systems examined contain a total of 500 molecules. The explicit compositions of the various cases examined are listed in Sec. 3.

2.3 Calculating the Dielectric Constant

As noted above, the more physically significant variable is the dielectric polarization P rather than the dielectric constant ε. There are two contributions to P that are to be obtained for H_2O, CO_2, and their mixtures.

The nonpolar part of P is obtained from the molar density, ρ_i, and the molecular polarizability, α_i, of the components by

$$P_{\mathrm{non}}=\frac{4\pi}{3}N_A\sum_i \alpha_i\rho_i, \quad (6)$$

where N_A is the Avogadro constant. We use values of the polarizability of 2.912×10^{-24} cm^3 for CO_2 [23] and 1.457×10^{-24} cm^3 for H_2O [45].

The polar contribution (which is zero for pure CO_2 since it has no permanent dipole moment) comes from the fluctuations in the total dipole moment of the ensemble of molecules. The quantity εpol is obtained from the simulations using the fluctuation expression appropriate for conducting boundary conditions for the electrostatics [46]:

$$\varepsilon_{\mathrm{pol}}=1+\frac{4\pi\left\langle \mathbf{M}^2\right\rangle}{3Vk_{\mathrm{B}}T}. \quad (7)$$

Here $<\boldsymbol{M}^2>$ is the long-time average value of the square of the total dipole moment of the fluid in a volume V at temperature T and kB is Boltzmann’s constant. $<\boldsymbol{M}^2>$ is determined in the simulation by evaluating at each time step $\mathrm{M}^2=\left(\sum_i \boldsymbol{\mu}_i\right)^2$ where $\boldsymbol{\mu}_i$ is the dipole moment vector of molecule *i*.

Next, one determines Ppol from Eq. 2:

$$P_{\mathrm{pol}}=\frac{(\varepsilon_{\mathrm{pol}}-1)\,(2\varepsilon_{\mathrm{pol}}+1)}{9\varepsilon_{\mathrm{pol}}} \quad (8)$$

The total polarization is then P = Pnon + Ppol. The dielectric constant is obtained by solving the Kirkwood relation, Eq. 2, for ε:

$$\varepsilon=\frac{1}{4}\left\{(1+9P)+\left[(1+9P)^2+8\right]^{1/2}\right\}. \quad (9)$$

3 Results

Simulations were performed for H_2O, CO_2, and their mixtures at temperatures of 700 K and 1000 K for pressures of 0.1 GPa, 0.3 GPa, 1 GPa, and 3 GPa. For these temperatures and pressures, mixtures were simulated with water mole fractions, xw, of 0.9, 0.75, 0.5, and 0.25.

3.1 Pure H_2O

The results from the H_2O simulations are reported in Table 2. The standard uncertainty for the molar density ρ is on the order of 0.1 % of the average value, while the standard uncertainty for the dielectric constant ε is on the order of 1 %.

Table 2 also shows the values calculated from the IAPWS correlations for ε [20,21] and for ρ [47,48]. While a close match is not necessary for our purpose of testing mixing rules, the qualitative agreement indicates that the SPC/E model is physically reasonable for the dielectric behavior of water at these conditions.

3.2 Pure CO_2

The results from the CO_2 simulations are reported in Table 3. The standard uncertainty for the molar density ρ is on the order of 0.1 % of the average value. Since the value of ε for CO_2 is calculated directly from the simulated density, its uncertainty is similar.

3.3 Mixtures

The results from the simulations of mixtures at water mole fractions, xw, of 0.9, 0.75, 0.5, and 0.25, are reported in Table 4. The standard uncertainty for the tabulated results is approximately the same as the uncertainty for pure H_2O as discussed in Sec. 3.1.

Because mixtures of water and CO_2 can undergo phase separation (which would distort the dielectric results) at some high-temperature, high-pressure conditions [49-51], we checked for signs of phase separation by examining the unlike pair distribution functions. No unusual compositional order was observed at any of the simulated conditions, indicating that the simulations were within the one-phase region.

4 Analysis of Mixing Rules

In Figs. 1-4, we plot the simulated dielectric constants from Table 4 for mixtures at pressures of 0.1 GPa, 0.3 GPa, 1 GPa, and 3 GPa, respectively. We also plot the values predicted by the different mixing rules discussed in Sec. 1.

For the mixing rules of Looyenga [24,25] (Eq. 1) and of Wang and Anderko [29] (Eq. 4), the mixture dielectric constant is obtained at any composition from knowledge of the pure-component values at the same temperature and pressure. Results from these two mixing rules can therefore be plotted as continuous curves on Figs. 1-4.

For the mixing rule of Oster [28] (Eq. 3), the mixture density is required; these mixture densities are taken from Table 4 and therefore only individual points are plotted. We note that, in order to provide a self-consistent test of the mixing rules, we must use the simulated densities of the molecular model, which may or may not accurately represent the densities of real H_2O–CO_2 mixtures.

The mixing rule of Harvey and Prausnitz [31] (Eq. 5) requires not only mixture densities but also pure-component dielectric constants computed at the temperature of interest and a density corresponding to the reduced density of the mixture. This required additional simulations on pure H_2O for each point, which were performed as described in Sec. 2. It also requires the critical volumes, which were taken from reference equations of state for H_2O [47] and CO_2 [52].

It is worth noting that, while the Oster and Harvey-Prausnitz mixing rules both required additional computations for the testing procedure in this paper (simulation of density, and also extra pure-H_2O simulations for the Harvey-Prausnitz rule), this would not be a problem in actual use. In practical application, one would have correlations for the pure-component dielectric constants as functions of temperature and density (such as that of IAPWS [20,21] or Sverjensky et al. [11] for water), and that would provide sufficient information for any of the mixing rules.

5 Discussion

The purpose of this work is to test mixing rules, not to provide quantitatively accurate dielectric constants for real H_2O–CO_2 mixtures. The important feature in Figs. 1-4 is therefore the way in which the simulation data and the various mixing rules interpolate between the pure-component endpoints.

Some patterns can be seen in the results. In all cases, the Looyenga mixing rule predicts a lower dielectric constant than the other approaches; this difference is more pronounced at 700 K than at 1000 K and also becomes more pronounced at higher pressures. The Wang-Anderko and Oster approaches give similar results (except at 1000 K and 0.1 GPa, which is the lowest-density state simulated), indicating that the excess volume of mixing is small for this molecular model at the conditions simulated.

None of the mixing rules quantitatively reproduces the simulated mixture behavior at all conditions. The Looyenga approach is fairly accurate at lower pressures, and does well at all pressures for low water mole fractions. However, it underestimates the mixture dielectric constant at higher pressures for xw = 0.90 and xw = 0.75. The three mixing rules that use a theory-based combination of the pure-component polarizations generally overpredict the dielectric constant, in most cases producing greater errors than the Looyenga rule. The Harvey-Prausnitz mixing rule is closer to the data than are the mixing rules of Wang and Anderko or of Oster, but the improvement is relatively small.

It is not surprising that mixing rules based on combining pure-component polarizations overestimate the dielectric constant for these mixtures. The dielectric constant of polar fluids is dominated by correlations among dipoles [27]. For water, this correlation is largely due to hydrogen bonding. It is plausible that nonpolar solutes such as CO_2 disrupt the hydrogen-bonding network, reducing the dielectric polarization of the remaining water from that in pure water. This disruption of hydrogen-bonding networks by CO_2 in high-temperature water has been observed in neutron-diffraction experiments at 673 K and 0.13 GPa [53]. More generally, both Oster [28] and Harvey and Prausnitz [31] observed that Eqs. (3) and (5), respectively, did not accurately predict the dielectric constant for polar/nonpolar mixtures.

As for the question of which mixing rule should be used in geochemical studies such as those in Ref. [19], unfortunately there is no clear best choice. Looyenga's mixing rule tends to be the least inaccurate, but it should be recognized that it will probably underestimate the mixture dielectric constant at high pressures at the water-rich end of the composition range, which is the region of most geochemical interest. It might be wise to perform geochemical computations that are sensitive to the mixture dielectric constant with both the Looyenga rule and the Harvey-Prausnitz rule, which seem to provide lower and upper bounds. Such calculations would give an indication of the uncertainty introduced by the uncertainty of the mixture dielectric constant.

Similar tests of dielectric-constant mixing rules could in principle be performed with *ab initio* models for H_2O–CO_2 mixtures, as has been done for pure H_2O [22]. This would be a difficult calculation, but might be feasible with modern supercomputers. It would be interesting to see whether such a different model for the system showed similar mixing behavior for the dielectric constant.

Acknowledgments

We thank Dr. Matthieu Galvez for bringing this problem to our attention and for helpful comments during the course of the work.

References

1. Helgeson HC, Kirkham DH. Theoretical prediction of the thermodynamic behavior of aqueous electrolytes at high pressures and temperatures: I. Summary of the thermodynamic/electrostatic properties of the solvent. Am. J. Sci. 1974; 274:1089–1198.
2. Helgeson HC, Kirkham DH. Theoretical prediction of the thermodynamic behavior of aqueous electrolytes at high pressures and temperatures: II. Debye-Hückel parameters for activity coefficients and relative partial molal properties. Am. J. Sci. 1974; 274:1199–1261.
3. Helgeson HC, Kirkham DH. Theoretical prediction of the thermodynamic behavior of aqueous electrolytes at high pressures and temperatures: III. Equation of state for aqueous species at infinite dilution. Am. J. Sci. 1976; 276:97–240.
4. Helgeson HC, Kirkham DH, Flowers GC. Theoretical prediction of the thermodynamic behavior of aqueous electrolytes at high pressures and temperatures: IV. Calculation of activity coefficients, osmotic coefficients, and apparent molal and standard and relative partial molal properties to 5 kb and 600 ℃C. Am. J. Sci. 1981; 281:1241–1516.
5. Tanger JC, Helgeson HC. Calculation of the thermodynamic and transport properties of aqueous species at high pressures and temperatures: revised equations of state for the standard partial molal properties of ions and electrolytes. Am. J. Sci. 1988; 288:19–98.
6. Johnson JW, Oelkers EH, Helgeson HC. SUPCRT92: a software package for calculating the standard molal thermodynamic properties of minerals, gases, aqueous species, and reactions from 1 to 5000 bars and 0 to 1000 ℃C. Comput. Geosci. 1992; 18:899–947.
7. Shock EL, Oelkers EH, Johnson JW, Sverjensky DA, Helgeson HC. Calculation of the thermodynamic and transport properties of aqueous species at high pressures and temperatures: effective electrostatic radii to 1000 ℃C and 5 kb. Faraday Soc. Trans. 1992; 88:803–826.
8. Dolejš D. Thermodynamics of aqueous species at high temperatures and pressures: equations of state and transport theory. Rev. Mineral. Geochem. 2013; 76:35–79.
9. Dolejš D, Manning CE. Thermodynamic model for mineral solubility in aqueous fluids: theory, calibration and application to model fluid-flow systems. Geofluids. 2010; 10:20–40.
10. Manning CE. Thermodynamic modeling of fluid-rock interaction at mid-crustal to upper-mantle conditions. Rev. Mineral. Geochem. 2013; 76:135–164.
11. Sverjensky DA, Harrison B, Azzolini D. Water in the deep Earth: The dielectric constant and the solubilities of quartz and corundum to 60 kb and 1200 ℃C. Geochim. Cosmochim. Acta. 2014; 129:125–145.
12. Facq S, Daniel I, Montagnac G, Cardon H, Sverjensky DA. In situ Raman study and thermodynamic model of aqueous carbonate speciation in equilibrium with aragonite under subduction zone conditions. Geochim. Cosmochim. Acta. 2014; 132:375–390.
13. Kerrick DM. Review of metamorphic mixed volatile (CO2-H2O) equilibria. Am. Mineralogist. 1974; 54:729–762.
14. Connolly JAD, Cesare B. C-O-H-S fluid composition and oxygen fugacity in graphitic metapelites. J. Metamorphic Geol. 1993; 11:379–388.
15. Huizenga JM. Thermodynamic modeling of C-O-H fluids. Lithos. 2001; 55:101–114.
16. Zhang C, Duan Z. A model for C-O-H fluid in the Earth's mantle. Geochim. Cosmochim. Acta. 2009; 73:2089–2102.
17. Walther JV. Ionic association in H2O-CO2 fluids at mid-crustal conditions. J. Metamorphic Geol. 1992; 10:789–797.
18. Akinfiev N, Zotov A. Thermodynamic description of equilibria in mixed fluids (H2O– non-polar gas) over a wide range of temperature (25-700℃C) and pressure (1-5000 bars). Geochim. Cosmochim. Acta. 1999; 63:2025–2041.
19. Galvez ME, Manning CE, Connolly JAD, Rumble D. The solubility of rocks in metamorphic fluids: a model for rock dominated conditions to upper mantle pressure and temperature with application to pelitic systems. Earth Planet. Sci. Lett. 2015 in press. doi:10.1016/j.epsl.2015.06.019.
20. International Association for the Properties of Water and Steam. Release on the Static Dielectric Constant of Ordinary Water Substance for Temperatures from 238 K to 873 K and Pressures up to

1000 MPa. 1997. http://www.iapws.org/relguide/Dielec.htmlhttp://www.iapws.org/relguide/Dielec.html

21. Fernández DP, Goodwin ARH, Lemmon EW, Levelt Sengers JMH, Williams RC. A formulation for the static permittivity of water and steam at temperatures from 238 K to 873 K at pressures up to 1200 MPa, including derivatives and Debye-Hückel coefficients. J. Phys. Chem. Ref. Data. 1997; 26:1125–1166.
22. Pan D, Spanu L, Harrison B, Sverjensky DA, Galli G. Dielectric properties of water under extreme conditions and transport of carbonates in the deep Earth. Proc. Nat. Acad. Sci. 2013; 110:6646–6650. [PubMed: 23513225]
23. Harvey AH, Lemmon EW. Method for estimating the dielectric constant of natural gas mixtures. Int. J. Thermophys. 2005; 26:31–46.
24. Looyenga H. Dielectric constants of heterogeneous mixtures. Physica. 1965; 31:401–406.
25. Looyenga H. Dielectric constants of homogeneous mixtures. Mol. Phys. 1965; 9:501–511.
26. Böttcher CJF. Theory of Electric Polarization. Elsevier, Amsterdam (2nd). 1973; 1
27. Kirkwood JG. The dielectric polarization of polar liquids. J. Chem. Phys. 1939; 7:911–919.
28. Oster G. The dielectric properties of liquid mixtures. J. Am. Chem. Soc. 1946; 68:2036–2041. [PubMed: 21001127]
29. Wang P, Anderko A. Computation of dielectric constants of solvent mixtures and electrolyte solutions. Fluid Phase Equilib. 2001; 186:103–122.
30. Orlov AG, Smirnov SN. Determining the phase equilibrium parameters of a binary mixture with a polar component from its dielectric constant. Thermal Eng. 1994; 41:650–654.
31. Harvey AH, Prausnitz JM. Dielectric constants of fluid mixtures over a wide range of temperature and density. J. Solution Chem. 1987; 16:857–869.
32. Berendsen HJC, Grigera JR, Straatsma TP. The missing term in effective pair potentials. J. Phys. Chem. 1987; 91:6269–6271.
33. Zhang Z, Duan Z. An optimized molecular potential for carbon dioxide. J. Chem. Phys. 2005; 122:214507. [PubMed: 15974754]
34. Pérez-Sánchez G, González-Salgado D, Piñiero MM, Vega C. Fluid-solid equilibrium of carbon dioxide as obtained from computer simulations of several popular potential models: The role of the quadrupole. J. Chem. Phys. 2013; 138:084506. [PubMed: 23464159]
35. Aimoli CG, Maginn EJ, Abreu CRA. Force field comparison and thermodynamic property calculation of supercritical CO2 and CH4 using molecular dynamics simulations. Fluid Phase Equilib. 2014; 368:80–90.
36. Potoff JJ, Siepmann JI. Vapor-liquid equilibria of mixtures containing alkanes, carbon dioxide, and nitrogen. AIChE J. 2001; 47:1676–1682.
37. Duan Z, Zhang Z. Equation of state of the H2O, CO2, and H2O-CO2 systems up to 10 GPa and 2573.15 K. Molecular dynamics simulations with ab initio potential surface. Geochim. Cosmochim. Acta. 2006; 70:2311–2324.
38. Hansen, JP.; McDonald, IR. Theory of Simple Liquids. 2nd. Academic Press; New York: 1986. p. 179
39. Kong CL. Combining rules for intermolecular potential parameters: II. Rules for the Lennard-Jones (12-6) potential and the Morse potential. J. Chem. Phys. 1973; 59:2464–2467.
40. Sangster MJL, Dixon M. Interionic potentials in alkalai halides and their use in simulations of the molten salts. Adv. Phys. 1976; 25:247–342.
41. Martyna GJ, Tobias DJ, Klein ML. Constant pressure molecular dynamics algorithms. J. Chem. Phys. 1994; 101:4177–4189.
42. Martys NS, Mountain RD. Velocity Verlet algorithm for dissipative-particle- dynamics-based models of suspensions. Phys. Rev. E. 1999; 59:3733–3736.
43. Evans DJ, Murad S. Singularity free algorithm for molecular dynamics simulation of rigid polyatomics. Mol. Phys. 1977; 34:327–331.
44. Hogg, RV.; McKean, JW.; Craig, AT. Introduction to Mathematical Statistics. 6th. Pearson Prentice Hall; Upper Saddle River, NJ: 2005.

45. Russell AJ, Spackman MA. Vibrationalaveragingofelectricalproperties. Development of a routine theoretical method for polyatomic molecules. Mol. Phys. 1995; 84:1239–1255.

46. Allen, MP.; Tildesley, DJ. Computer Simulation of Liquids. Clarendon Press; Oxford: 1987. p. 163

47. Wagner W, Pruβ A. The IAPWS formulation 1995 for the thermodynamic properties of ordinary water substance for general and scientific use. J. Phys. Chem. Ref. Data. 2002; 31:387–535.

48. International Association for the Properties of Water and Steam. Revised Release on the IAPWS Formulation 1995 for the Thermodynamic Properties of Ordinary Water Substance for General and Scientific Use. 2014. http://www.iapws.org/relguide/IAPWS- 95.htmlhttp://www.iapws.org/relguide/IAPWS- 95.html

49. Tödheide K, Franck EU. Das Zweiphasengebiet und die kritische Kurve im System Kohlendioxid–Wasser bis zu Drucken von 3500 bar. Z. Phys. Chem., Neue Folge. 1963; 37:387–401.

50. Mather AE, Franck EU. Phase equilibria in the system carbon dioxide–water at elevated pressures. J. Phys. Chem. 1992; 96:6–8.

51. Holland R, Powell R. Activity-composition relations for phases in petrological calculations: an asymmetric multicomponent formulation. Contrib. Mineral. Petrol. 2003; 145:492–501.

52. Span R, Wagner W. A new equation of state for carbon dioxide covering the fluid region from the triple-point temperature to 1100 K at pressures up to 800 MPa. J. Phys. Chem. Ref. Data. 1996; 25:1509–1596.

53. Botti A, Bruni F, Mancinelli R, Ricci MA, Lo Celso F, Triolo R, Ferrante F, Soper AK. Study of percolation and clustering in supercritical water-CO_2 mixtures. J. Chem. Phys. 2008; 128:164504. [PubMed: 18447456]

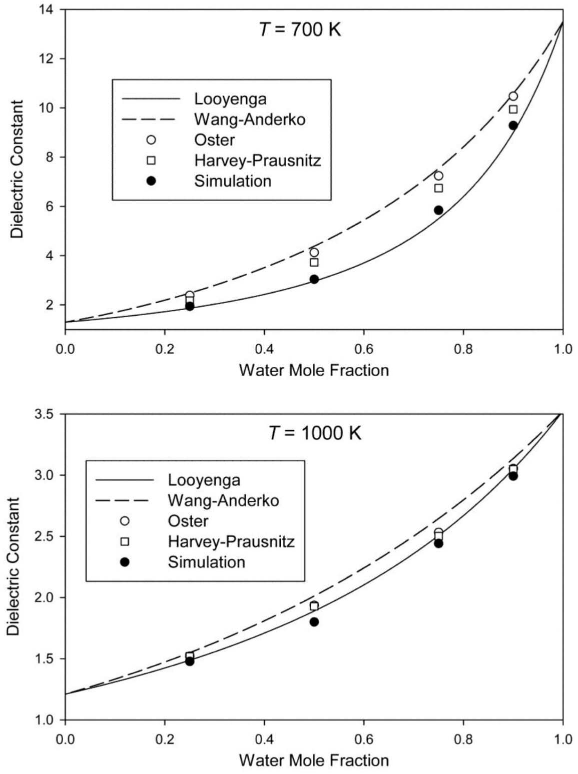

Fig. 1.

Mixture dielectric constant from molecular simulation at a pressure of 0.1 GPa compared to predictions of various mixing rules

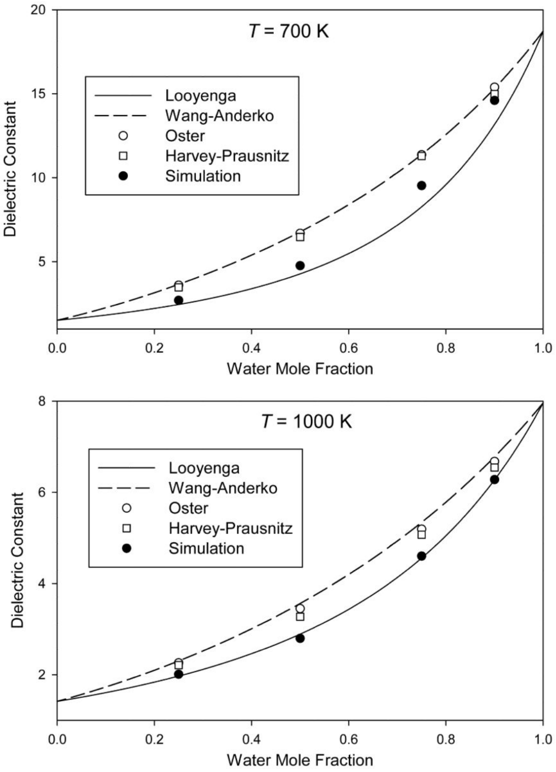

Fig. 2.

Mixture dielectric constant from molecular simulation at a pressure of 0.3 GPa compared to predictions of various mixing rules

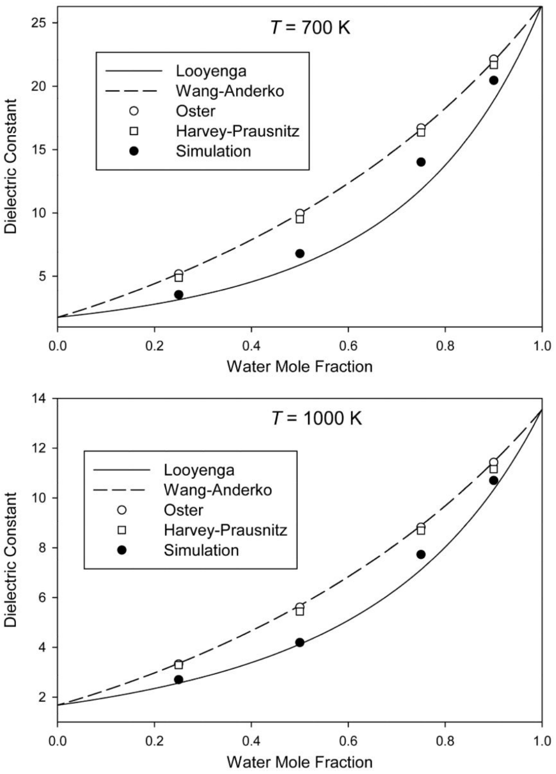

Fig. 3.

Mixture dielectric constant from molecular simulation at a pressure of 1.0 GPa compared to predictions of various mixing rules

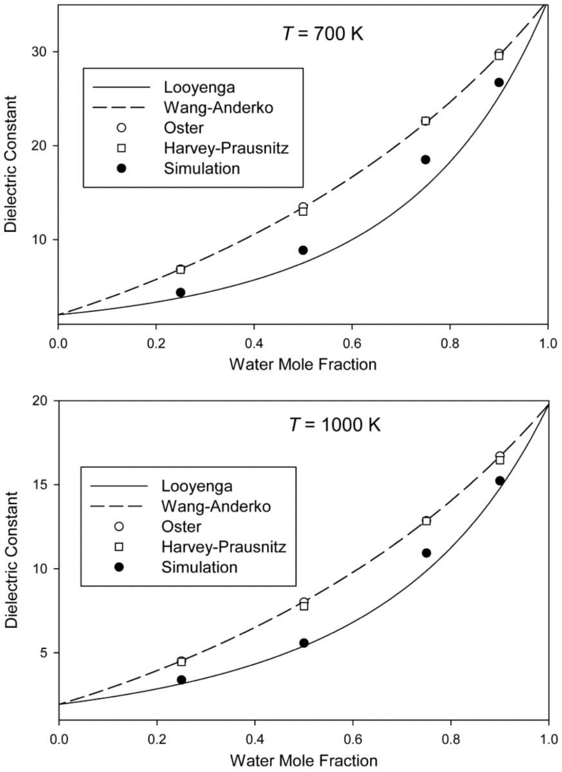

Fig. 4.

Mixture dielectric constant from molecular simulation at a pressure of 3.0 GPa compared to predictions of various mixing rules

Table 1

Lennard-Jones parameters and partial charges for H_2O [32], CO_2 [33], and the H_2O–CO_2 interaction [37]

Site	ε_{LJ}, kJ·mol^{-1}	σ, Å	q, e
	H_2O		
O	0.65	3.1657	−0.8476
H	0.0		0.4238
	CO_2		
C	0.2404	2.7918	0.5888
O	0.6888	3.00	−0.2944
	H_2O–CO_2		
C–OW	0.2937	3.1156	
OC–OW	0.5500	3.0297	
C–H	0.3004	2.8142	
OC–H	0.3932	2.1942	

Table 2

Simulation results for H_2O

T, K	**p, GPa**	**ρ, mol·cm $^{-3}$**	**ε**	**ρ_{IAPWS}, mol·cm^{-3}**	**$\varepsilon_{\text{IAPWS}}$**
700	0.1	0.03431	13.51	0.03618	13.75
	0.3	0.04515	18.70	0.04612	19.93
	1.0	0.05785	26.45	0.05794	28.60
	3.0	0.07192	35.49	0.07164	43.94
1000	0.1	0.01509	3.525	0.01473	2.956
	0.3	0.03233	7.956	0.03312	8.250
	1.0	0.04998	13.56	0.05061	15.72
	3.0	0.06656	19.79	0.06684	26.09

Table 3

Simulation results for CO_2

T, K	p, GPa	ρ, mol·cm $^{-3}$	ε
700	0.1	0.01251	1.299
	0.3	0.02079	1.517
	1.0	0.02954	1.761
	3.0	0.03788	2.002
1000	0.1	0.009007	1.211
	0.3	0.01704	1.416
	1.0	0.02659	1.677
	3.0	0.03565	1.937

Table 4

Simulation results for H_2O–CO_2 mixtures

T, K	p, GPa	ρ, mol·cm $^{-3}$	ε
	$x_w = 0.9$		
700	0.1	0.02889	9.285
	0.3	0.04060	14.60
	1.0	0.05312	20.46
	3.0	0.06642	26.72
1000	0.1	0.01364	2.992
	0.3	0.02918	6.279
	1.0	0.04582	10.70
	3.0	0.06132	15.23
	$x_w = 0.75$		
700	0.1	0.02287	5.842
	0.3	0.03486	9.526
	1.0	0.04696	14.01
	3.0	0.05922	18.50
1000	0.1	0.01211	2.441
	0.3	0.02556	4.600
	1.0	0.04062	7.724
	3.0	0.05466	10.93
	$x_w = 0.5$		
700	0.1	0.01704	3.036
	0.3	0.02804	4.766
	1.0	0.03909	6.782
	3.0	0.04981	8.864
1000	0.1	0.01051	1.800
	0.3	0.02142	2.797
	1.0	0.03424	4.189
	3.0	0.04623	5.580
	$x_w = 0.25$		
700	0.1	0.01401	1.942
	0.3	0.02361	2.704
	1.0	0.03351	3.545
	3.0	0.04295	4.374
1000	0.1	0.009533	1.478
	0.3	0.01876	2.009
	1.0	0.02975	2.700
	3.0	0.04013	3.386